Aspects of Thin-Film Superlattice Thermoelectric Materials, Devices, and Applications

Harald Böttner, Gang Chen, and Rama Venkatasubramanian

Abstract

Superlattices consist of alternating thin layers of different materials stacked periodically. The lattice mismatch and electronic potential differences at the interfaces and resulting phonon and electron interface scattering and band structure modifications can be exploited to reduce phonon heat conduction while maintaining or enhancing the electron transport. This article focuses on a range of materials used in superlattice form to improve the thermoelectric figure of merit.

Keywords: *thermal conductivity, thermoelectricity.*

Introduction

Ideas in using superlattices to improve the thermoelectric figure of merit (ZT) through the enhancement of electronic conductivity and reduction of phonon thermal conductivity were first discussed in a workshop by M.S. Dresselhaus, T. Harman, and R. Venkatasubramanian.[1] Subsequent publications from Dresselhaus's group on the quantum size effects on electrons drew wide attention and inspired intense research, both theoretical and experimental, on the thermoelectric properties of quantum wells and superlattices.[2] Several groups reported in recent years enhanced ZT in various superlattices such as Bi_2Te_3/Sb_2Te_3 and Bi_2Te_3/Bi_2Se_3,[3] and PbSeTe/PbTe quantum dot superlattices[4] (Figure 1). The large improvements observed in these materials systems compared with their parent materials are of great importance for both fundamental understanding and practical applications.

Superlattices are anisotropic. Different mechanisms to improve ZT along directions both parallel (in-plane) and perpendicular (cross-plane) to the film plane have been explored. Along the in-plane direction, potential mechanisms to increase ZT include quantum size effects that improve the electron performance by taking advantage of sharp features in the electron density of states,[2] and reduction of phonon thermal conductivity through interface scattering.[5] Along the cross-plane direction, one key idea is to use interfaces for reflecting phonons while transmitting electrons (phonon-blocking/electron-transmitting),[6] together with other mechanisms, such as electron energy filtering[7] and thermionic emission,[8] to improve electron performance. These mechanisms have been explored through a few superlattice systems whose constituent materials have reasonably good thermoelectric properties to start with, V–VI materials such as Bi_2Te_3/Sb_3Te_3,[3,9] IV–VI materials such as PbTe/PbSe,[4,9] and V–V materials such as Si/Ge[10–12] and Bi/Sb,[13] with the most impressive results obtained in Bi_2Te_3 superlattices[3] and PbTe-based quantum dot superlattices.[4]

The large ZT improvements observed in these superlattices shattered the $ZT \sim 1$ ceiling that persisted until the 1990s, opening new potential applications in cooling and power generation using solid-state devices. Much research is needed in materials, understanding, and devices to further advance superlattice thermoelectric technology. In this short article, we will give a summary of the past work, emphasizing the materials aspects of superlattices, while commenting on current understanding or lack of it, and some aspects of the device research. We refer to other review articles for more in-depth discussions on these topics.[5,6,14–19]

Materials and Properties

The work on quantum well and superlattice-based thermoelectric materials mostly focused on perfect (i.e., epitaxial) layer systems. So it was not surprising that, due to the extensive worldwide experience in IV–VI epitaxy,[20,21] approaches were taken to use this material system to prove the quantum confinement as well as the acoustic phonon scattering.[4,9] As Bi_2Te_3-based materials have the highest ZT around room temperature, successful efforts were started to develop suitable epitaxial systems for the V–VI compound family.[9,22] It is worth mentioning that both IV–VI and V–VI semiconductor material families have a useful structural relationship (Figures 2a and 2b).[23] The current thin-film device technologies for IV–VI and V–VI compounds use either one or the other of these two material systems. Mixed staggered IV–V/V–VI superlattice thin-film devices are not known so far.

V–VI Superlattices

Venkatasubramanian and co-workers reported Bi_2Te_3-based superlattices grown by metallorganic chemical vapor deposition (MOCVD) on GaAs substrates.[22] The GaAs substrates were chosen for their ease of cleaning prior to epitaxial deposition and the fact that substrates with 2–4° misorientation with respect to ⟨100⟩ can be conveniently obtained. It is important to note that these trigonal-structured Bi_2Te_3 materials are grown on GaAs with fcc structure. The misorientation allows the

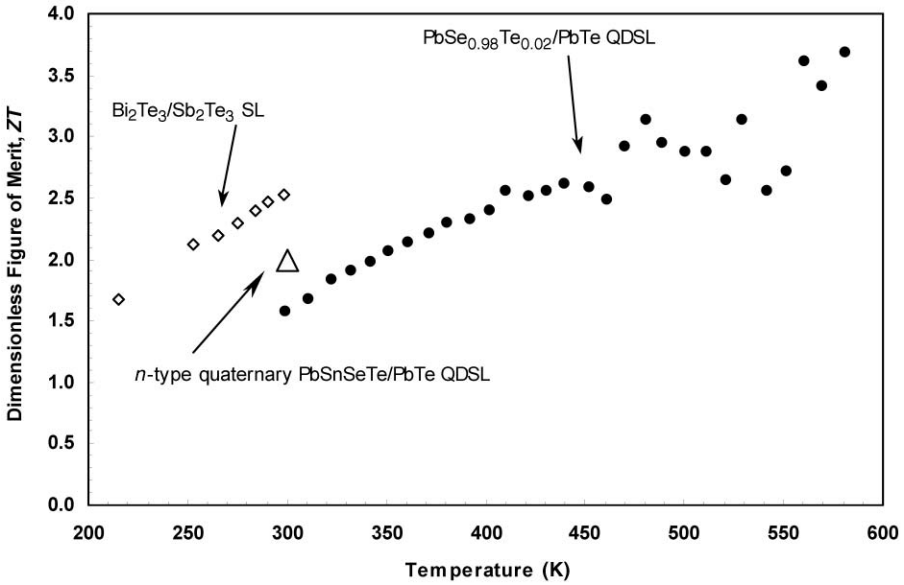

Figure 1. Thermoelectric figure of merit ZT for Bi_2Te_3/Sb_2Te_3 superlattices[3] (SL), PbSnSeTe/PbTe quantum dot superlattices (QDSL), and PbTeSe/PbTe quantum dot superlattices.[4,45]

initiation of the epitaxial process at the kink sites on the surface, thereby allowing the growth of mismatched materials. The growth of Bi_2Te_3-based materials, with the rather weak van der Waals bonds along the growth direction, requires a low-temperature process. A low-temperature growth process leads to high-quality, abrupt superlattice interfaces with minimal interlayer mixing, and also allows the growth of highly lattice-mismatched materials systems without strain-induced three-dimensional islanding. Figure 3 shows a high-resolution transmission electron micrograph of a Bi_2Te_3/Sb_2Te_3 superlattice on a GaAs substrate, delineating the two very different crystalline orientations. *In situ* ellipsometry has been used to gain further nanometer-scale control over deposition.[24]

As V–VI epitaxy is rather a scientific "virgin soil," it is not surprising that even for the single homogeneous V–VI layers of the central compound Bi_2Te_3, only minimal information regarding thin-film deposition and thermoelectric property characterization can be found. The problem of a low Te sticking coefficient is discussed in Reference 25. Different film growth methods based on MBE,[9,25–27] MOCVD,[22] flash evaporation,[28–30] and co-evaporation[31,32] have been used to grow single layers and superlattices on various substrates. Nurnus et al.[23] used a rather high deposition temperature compared with that used in MOCVD but were still able to obtain high-quality $(Bi_2Te_3)/Bi_2(Te,Se)_3$ superlattices using element sources. The power factor ($PF = \alpha^2/\rho\kappa$) of 50 μW cm^{-1} K^{-2} reported in Reference 33 for Bi_2Te_3 is close to that of the best single crystals, which is 57 μW cm^{-1} K^{-2}.[34] Unfortunately, the mobility is limited to ~150 cm^2 V^{-1} s^{-1}. A critical item in maintaining the outstanding *ZT* of superlattices is their stability against cation (*p*-material) and anion (*n*-material) interdiffusion. Results reported by Nurnus et al.[23,33] strongly indicate a dependence of the superlattice stability against diffusion on perfection of the layer structure.

Recently, sputtering as a new deposition method for forming V–VI superlattices[35] was tested. Starting with alternating element layers, the corresponding superlattice thermoelectric compounds were formed by a subsequent annealing procedure. Here, at lower temperatures, the anions in the *n*-("Se/Te") alloy system or the cations in the *p*-("Bi/Sb") alloy system tend to interdiffuse while compounding the thermoelectric material. Taking into account the results by Johnson,[36] who succeeded in forming superlattices in the V–VI materials system using "modulated elemental reactants," it can be concluded that besides alternating layers, a necessary condition for the formation of superlattices is to deposit layers that are as perfectly oriented as possible in order to obtain optimum diffusion stability for reliable final devices. For the case of perfect *c*-oriented layers, the fast diffusion paths are

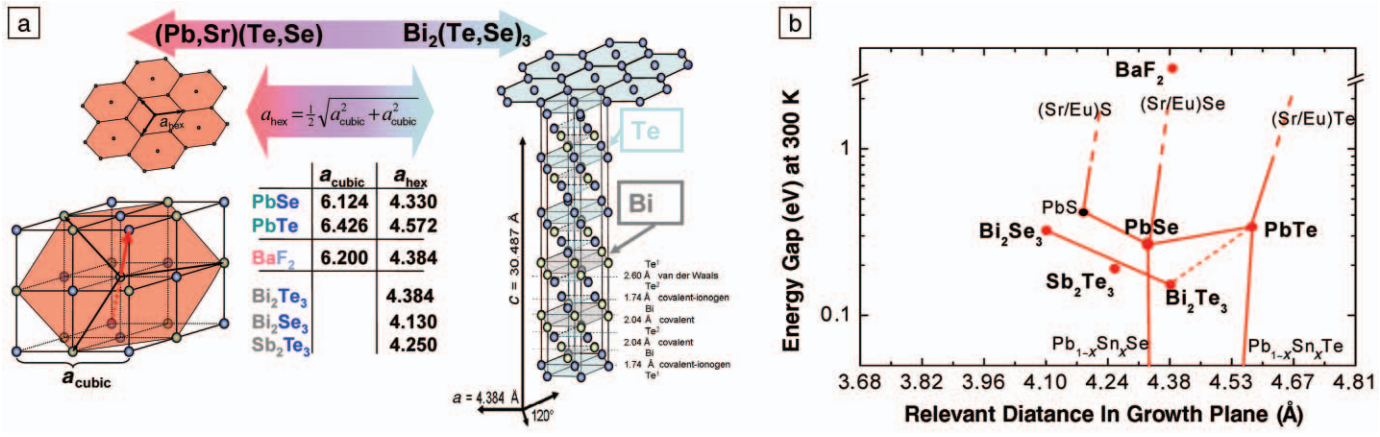

Figure 2. (a) Crystallographic data for IV–VI and V–VI compounds, highlighting the structural relationship between both material systems. (b) Epitaxial map of semiconductor materials (at room temperature) that could be suitable in combination with Bi_2Te_3, based on their relevant atomic distance with respect to the a-plane of Bi_2Te_3.

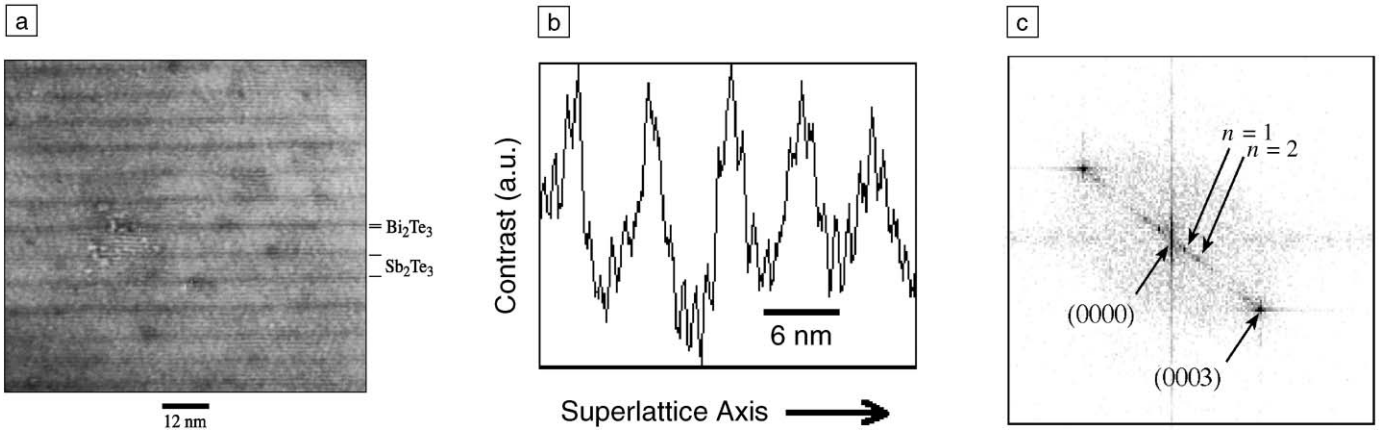

Figure 3. (a) Transmission electron micrograph of a Bi_2Te_3/Sb_2Te_3 (10 Å/50 Å) superlattice. (b) Image contrast oscillations through the superlattice. (c) Fast Fourier transform of the image in (a), showing the superlattice reflections of order n.[22]

blocked, even in the case of the non-epitaxially arranged layers, according to Johnson's work.[36] If the interdiffusion is blocked in the *a*-plane, superlattices will be stable until the intrinsic interdiffusion in the *c*-direction is activated at significantly higher temperatures. For the V–VI compounds, it is well known that the interdiffusion coefficients in the *c*-direction are normally smaller, by decades, than in the *a*-direction.[37]

The *ZT* values of V–VI-based superlattices can be measured in either in-plane or cross-plane directions. So far, the largest enhancement is in the cross-plane direction, with the major gain coming from the thermal conductivity reduction. Venkatasubramanian reported a cross-plane $ZT \sim 2.4$ at room temperature for the *p*-type Bi_2Te_3-Sb_2Te_3 superlattices with a period of ~6 nm.[4] In such superlattices, the electronic power factor is in the range of 40 μW cm^{-1} K^{-2} to 60 μW cm^{-1} K^{-2}, comparable to or higher than standard bulk *p*-type Bi_2Te_3 solid-solution alloys measured along the *a*–*b* axis. However, the phonon thermal conductivity (κ_p) dropped to 0.22 W/m K, about a factor of 5 lower than that of bulk alloys along *a*–*b* axis. Lambrecht et al.[38] determined an in-plane reduction of the total thermal conductivity (electrons and phonons) down to 65%, compared with homogenous Bi_2Te_3 for *n*-type $Bi_2Te_3/Bi_2(Se_{0.12}Te_{0.88})_3$ superlattices with a 10-nm period.

IV–VI Superlattices

IV–VI nanolayers have been successfully grown for more than a decade for IV–VI infrared lasers.[39] Because of its physical and chemical properties, the IV–VI materials system is relatively easy to handle, compared with the V–VI compounds, particularly for epitaxial growth. Thus, a lot of literature can be found on the growth details and layer properties of IV–VI nanolayer stacks.[40,41] Here, we summarize results exclusively focused on thermoelectric applications.

The initial effort in IV–VI systems was focused on electron confinement effects. Using MBE-grown $PbTe/Eu_xPb_{1-x}Te$, Harman and co-workers showed an increased electron power factor ($\alpha^2\sigma$) inside the quantum wells along the in-plane direction,[42,43] as predicted by Hicks and Dresselhaus. However, the barriers in multiple quantum wells (MQWs) degrade the overall *ZT*, because they conduct heat without contributing to electron performance. Harman and co-workers further explored various IV–VI superlattices. They found that in PbTe/Te superlattices, obtained by the addition of a few nanometers of Te above the PbTe layer, *ZT* increased from 0.37 to 0.52 at room temperature, and this increase was associated with the formation of quantum dot structures at the interface.[44] The Harman group further discovered experimentally that quantum dot superlattices based on $PbTe/PbSe_xTe_{1-x}$ (with $x \sim 0.98$) have an even higher *ZT*.[45] The quantum dot formation is due to the lattice mismatch between PbTe and PbSeTe[40] (Figure 4). PbTe-based quantum dot superlattices with a total thickness of 100–200 μm have been grown with good thermoelectric properties along the in-plane direction.[4] PbTe/PbSeTe *n*-type quantum dot superlattices were obtained by Bi doping, and *p*-type quantum dot superlattices were obtained through Na doping. The best bulk PbTe-based alloys have a room temperature *ZT* of ~0.4. Harman et al.[4] reported *n*-type PbTe/PbSeTe quantum dot superlattices with $ZT = 1.6$ at room temperature, compared with $ZT \sim 0.4$ in the best bulk PbTe alloys, and inferred that quaternary superlattices based on PbTe/PbSnSeTe have a room temperature *ZT* of ~2. For the ternary PbTe/PbSeTe superlattices, the factor of 4 increases come mainly from a large reduction in the thermal conductivity, while the power factor remains similar to that of the bulk, albeit at different optimum carrier concentrations. The combined electron and phonon thermal conductivity ($\kappa_e + \kappa_p$) drops from bulk values of ~2.5 W/m K to 0.5 W/m K. Considering that the electronic contribution to thermal conductivity for both superlattices and bulk materials is ~0.3 W/m K, a significant phonon thermal conductivity reduction is obvious.

Böttner and co-workers studied the in-plane thermoelectric properties of *n*- and *p*-doped $PbTe/PbSe_{0.20}Te_{0.80}$ systems.[9,46] Compared with corresponding bulk $PbSe_xTe_{1-x}$ material, a significant reduction in the thermal conductivity parallel to the growth direction was measured. Together with nearly unchanged power factors, an in-plane *ZT* enhancement of up to 40% at

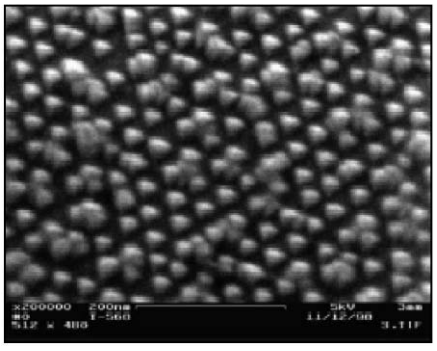

Figure 4. Quantum dot structures in the PbTe/PbSeTe system.[42]

a temperature of 500 K was estimated. Recently, Caylor et al.[47] reported their effort in growing PbTe/PbSe superlattices.

Other Superlattice Systems

Nurnus and co-workers studied IV–VI/V–VI heteroepitaxial layers to evaluate quantum confinement in V–VI layers using suitable "wide-bandgap" IV–VI alloys such as $Bi_2Te_3/Pb_{1-x}Sr_xTe$,[33,48] including results involving stability against annealing. The practical use of the concept (Figure 2) of a structural relationship between IV–VI and V–VI compounds was recently proved by Caylor et al., who deposited Bi_2Te_3 on a standard GaAs substrate as a buffer layer, followed by a IV–VI superlattice.[47] They found out, surprisingly, that superlattices in (111) and (100) orientations grow simultaneously at lower temperatures.

Other superlattice systems have been studied for their thermoelectric properties, such as Si/Ge superlattices,[10–12] Bi/Sb superlattices,[13] and skutterudite-based superlattices.[49] Si/Ge and Si/SiGe alloy superlattices have shown a large reduction in thermal conductivity compared with that of homogeneous alloys in the cross-plane direction,[10,11] while in the in-plane direction, thermal conductivity values are comparable with that of the homogeneous alloy with equivalent composition to the superlattices.[50] Despite the reduction in thermal conductivity, there are no conclusive results on the figure of merit because of difficulties in measuring the thermoelectric properties of very thin films. Reported measurements of the thermoelectric properties of Bi/Sb and skutterudite superlattices are scarce and not conclusive.[51,52]

Characterization of Thermoelectric Properties

Thermoelectric property measurements in many cases have been the bottleneck in the development and understanding of superlattice-based materials.[53] Because of anisotropy, all thermoelectric properties, including the Seebeck coefficient α, electrical conductivity σ, and thermal conductivity κ, should be measured in the same direction and, ideally, on the same sample. Along the in-plane direction, thermal conductivity is usually the most difficult parameter to measure. However, the substrate and the buffer layers can also easily overwhelm the Seebeck coefficient and electrical conductivity measurements. The need to isolate the properties of the film from those of the substrate and the buffer layer often influences the choice of the substrate and the film thickness in the growth of superlattices. In the cross-plane direction, the 3ω method and the pump-and-probe method are often used to measure the thermal conductivity of superlattices.[54,55] However, measuring the Seebeck coefficient and the electrical conductivity in the cross-plane direction can be even more challenging. Venkatasubramanian et al.[3] adapted the transmission line model (TLM) technique used for the measurement of specific electrical contact resistivities (ρ_c) to determine the cross-plane electrical resistivities in Bi_2Te_3-based superlattices, which is feasible when ρc is smaller than the specific internal resistance of the thermoelectric film d/σ, where d is the thickness of the superlattice film.

Besides individual property measurements to determine ZT, other methods for direct ZT determination have been successful. Venkatasubramanian et al.[3] adapted the Harman method[56] to determine ZT in the cross-plane direction of Bi_2Te_3-based superlattices with a maximum thickness of the superlattice up to 5 μm. Yet the most unambiguous measurement of the enhanced ZT comes from direct measurements of the cooling effect. Harman used this method to characterize the performance of his PbTe/PbSeTe quantum dot superlattices.[4] He measured cooling based on a thermocouple with one leg made of the superlattice and the other leg made of a section of Au wire, properly matched in length. The maximum cooling measured from such a thermocouple was 43.7 K, while a similar couple made of the best bulk thermoelectric material only reached 30.8 K. To make such a couple, the total thickness of his superlattice sample was ~100 μm.

Current Understanding

Experimental results so far have shown that the thermal conductivity reduction was mainly responsible for ZT enhancement in the superlattices. Theoretical studies on the thermal conductivity have been carried out.[16,17] These models generally fall into two different camps.

The first group treats phonons as incoherent particles and considers interface scattering as the classical size effect that is analogous to the Casimir limit at low temperatures in bulk materials and Fuchs–Sonderheim treatment of electron transport.[57–59] These classical size effect models assume that interface scattering is partially specular and partially diffuse, and can explain experimental data for superlattices in the thicker period limit.

The other group of models is based on the modification of phonon modes in superlattices, considering the phonons as totally coherent.[60,61] In superlattices, the periodicity has three major effects on the phonon spectra: (1) phonon branches fold, owing to the new periodicity in the growth direction; (2) mini-bandgaps form; and (3) the acoustic phonons in the layer with a frequency higher than that in the other layer become flat or confined because of the mismatch in the spectrum. Comparison with experimental data, however, shows that the group velocity reduction alone is insufficient to explain the magnitude of the thermal conductivity reduction perpendicular to the film plane, and it fails completely to explain the thermal conductivity reduction along the film plane.[61,62] The reason is that the lattice dynamics model assumes phase coherence of the phonons over the entire superlattice structure and does not include the possibility of diffuse interface scattering, which destroys the perfect phase coherence picture. Partially coherent phonon transport models can capture the trend of thermal conductivity variation in both the in-plane and the cross-plane directions over the entire thickness range.[63,64] Molecular dynamics simulations considering interface mixing can generate trends similar to that observed experimentally on GaAs/AlAs superlattices, which is consistent with the modeling.[65] Past models of thermal conductivity focused on III–V and IV–IV superlattices. There are no detailed models on IV–VI and V–VI superlattices. Venkatasubramanian et al.[66] observed a minimum in thermal conductivity for Bi_2Te_3-based superlattices at a periodic thickness of ~6 nm. Although similar trends can be obtained from partially coherent phonon-transport models, the minima based on such models typically occur around 3–5 monolayers (i.e., 1–2 nm).[63,64] The discrepancy could be due to the unusually large unit cell in the c-axis direction and potentially to interface mixing, which is not well included in current models, and to phonon localization.[66] The modeling conclusion that coherent states of phonons cannot reproduce experimental data has significant implications for materials synthesis, suggesting that other nanostructures can lead to similar results.[67]

While the thermal conductivity reduction has been largely responsible for the reported high ZT so far in IV–VI and V–VI superlattices, the importance of maintaining the electronic power factor cannot be overemphasized. Although in both these systems, the maximum power factors are close to those of their bulk counterparts, the optimal dopant concentrations between bulk and superlattice samples differ, at least in PbTe-based systems.[44,45] The bandgaps of the constituent

materials in the IV–VI and V–VI superlattices with high ZT are similar, suggesting that quantum size effects may not be important. However, small band-edge offsets can have an effect on the electron scattering mechanisms and shift the optimal carrier concentration. Although quantum size effects may not dominate in these materials systems, the principle of using quantum size effects to improve electron performance is sound. Minimizing interface scattering of electrons is crucial for realizing a high power factor. Better materials synthesis can potentially lead to structures that can take advantage of both increased electron performance and reduced phonon thermal conductivity.

Devices and Applications

The fabrication of superlattice-based devices can take advantage of many of the standard tools of semiconductor device manufacturing, such as photolithography, electroplating, wafer dicing, and pick-and-place systems. This allows scalability of the module fabrication, from simple modules that can pump milliwatts of heat to multiconnected module arrays. Both in-plane and cross-plane devices are under development, and each have their unique advantages, challenges, and applications.

Cross-plane superlattice-based devices typically have configurations similar to those of bulk thermoelectric modules, albeit with significantly shorter legs and smaller leg cross sections.[3,68] Such devices have extremely rapid cooling or heating characteristics, and fully functional devices can be built using 1/40,000 of the active material required for state-of-the-art bulk thermoelectric technology. Venkatasubramanian and co-workers have developed wafer-bonding technology to fabricate Bi_2Te_3 superlattice thermoelectric devices.[68] It is clear from such device development that significant challenges exist in translating the intrinsically high ZT of the materials to the high performance of the devices. Some of the issues are related to the significant electrical and thermal parasitic resistances in a modular assembly. First, the specific electrical contact resistance ρ_c at both ends of the p-type and n-type devices must be minimized such that ρ_c is much smaller than the specific resistance d/σ of the leg. Another significant challenge is the thermal management at both the hot and the cold sides, as the heat flux through each leg can be as large as ~1000 W/cm^2. Such a high heat flux cannot be handled with usual convective cooling techniques. Heat spreading by using sparsely spaced elements or advanced thermal management methods is necessary.

Cross-plane superlattice-based devices are being considered for a variety of applications. Thermoelectric coolers have long been used for the wavelength stability of semiconductor lasers. Currently used thermoelectric coolers are based on bulk materials machined down to small sizes (~2 mm × 2 mm × 1 mm). Superlattice-based devices can better match the footprint and heat flux of semiconductor lasers with a lower profile, which is extremely important for fitting into the existing packages such as metal transistor outline cans. Superlattice thermoelectric technology is also now being actively considered for the thermal management of hot-spot and transistor off-state leakage current in advanced microprocessors.

Besides cooling applications, superlattice-based thermoelectric devices can also be used for power-conversion applications. Figure 5 shows an example of local heating and cooling that can be realized with superlattice-based devices. Early studies carried out by Venkatasubramanian and co-workers of power-conversion efficiency using single p–n couples have shown a significant correlation with the measured ZT in the "inverted" p–n couples[69] by the Harman method.

In-plane device configurations are used mainly for sensors, and most of the past work has been based on polycrystalline thermoelectric material.[70,71] Superlattices with high ZT can improve the performance of these devices. For sensor applications, thermal bypass through the substrate must be minimized by removing the substrate, transferring the superlattice film to another low-thermal-conductance substrate, or depositing the film directly on a low-thermal-conductivity substrate.[71]

One big question regarding superlattice-based thermoelectric coolers and power generators is their stability and reliability. These devices operate under high heat and current fluxes, and both thermo- and electromigration are of great concern. At this stage, only a little work has been done. Venkatasubramanian's group[72] carried out initial power-cycle testing on relatively simple superlattice couples using $Pb_{37}Sn_{63}$ bonding for flip-chip attachment. No degradation in ΔT was observed after more than 100,000 power cycles, suggesting an intrinsic reliability in the superlattice material. However, the high-temperature reliability of superlattice materials has not been studied.

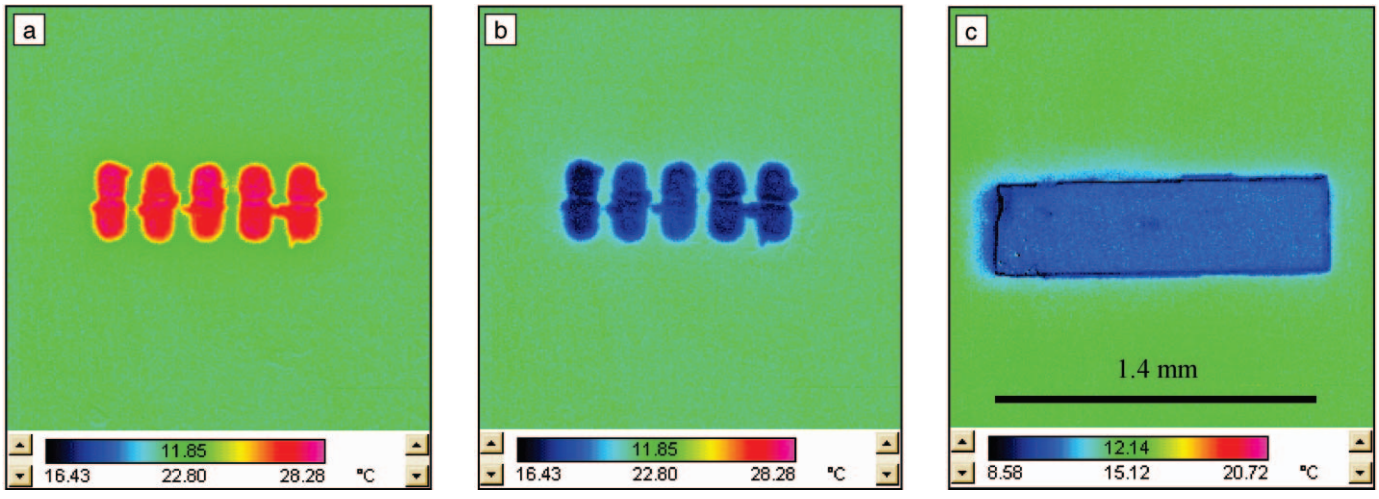

Figure 5. Infrared image of a row of five Bi_2Te_3-based thermoelectric superlattice microcoolers. (a) Discrete heating; (b) discrete cooling. (c) Combined discrete cooling devices for larger-area cooling. The scale marker in (c) applies to all three images.

Summary and Research Needs

The large figure-of-merit enhancements observed in V–VI- and IV–VI-based superlattices and quantum dot superlattices have an impact on both fundamental understanding and practical applications. For a long time, the maximum ZT for all bulk materials was limited to $ZT = 1$, and as a consequence, applications have been limited to niche areas. Progress made in superlattice-based thermoelectric materials show that $ZT = 1$ is not a theoretical limit. With the availability of high-ZT materials, many new applications will emerge. The progress made also calls for more effort in materials development, theoretical understanding, and device fabrication, concurrent with the pursuit of practical applications of these materials.

Materials-wise, research in both enhancing ZT and reducing cost is needed. Practical thermoelectric devices need both *n*-type and *p*-type materials with comparable figures of merit. So far, *p*-type Bi_2Te_3/Sb_2Te_3 superlattices have much higher ZT values than *n*-type Bi_2Te_3/Bi_2Se_3 superlattices, while PbTe/PbSeTe-based *n*-type and *p*-type quantum dot superlattices have comparable ZT values. Continuous improvements in ZT for different materials in different temperature ranges are needed. In addition to reducing the phonon thermal conductivity, the principle of increasing ZT through quantum confinement of electrons should be exploited, including the exploration of one-dimensional nanowires and nanowire superlattices.[73] Further reductions in thermal conductivity may be possible in aperiodic superlattices. Similar effects that lead to a reduction in phonon thermal conductivity may be observed in other nanostructures that are more amenable to mass production. In addition to materials development, theoretical studies are needed to further understand the electron and phonon thermoelectric transport. Particularly, quantitative tools capable of predicting thermoelectric transport properties are needed. While ZT has reached high values in superlattices, devices made of these materials have not reached the best performance of bulk thermoelectric coolers, due to difficulties in electrical contacts, heat spreading, materials matching, and fabrication. Continued progress in the device area is critical for translating the laboratory work successfully into practical applications.

Acknowledgments

H. Böttner's work was partially supported by the German Federal Ministry of Education and Research (BMBF), grant 03N2014A. G. Chen's work on superlattices was supported by the National Science Foundation and the Office of Naval Research MURI program. R. Venkatasubramanian's work was supported by DARPA/DSO through the Office of Naval Research (1997–present) and the Army Research Office (2000–2003).

References

1. *Proc. 1st Natl. Thermogenic Cooler Workshop*, edited by S.B. Horn (Center for Night Vision and Electro-Optics, Fort Belvoir, VA, 1992).
2. D. Hicks and M.S. Dresselhaus, *Phys. Rev. B* **47** (1993) p. 12727.
3. R. Venkatasubramanian, E. Siivola, T. Colpitts, and B. O'Quinn, *Nature* **413** (2001) p. 597.
4. T.C. Harman, P. Taylor, M.P. Walsh, and B.E. LaForge, *Science* **297** (2002) p. 2229.
5. G. Chen, *Semicond. Semimetals* **71** (2001) p. 203.
6. R. Venkatasubramanian, *Semicond. Semimetals* **71** (2001) p. 175.
7. B. Moyzhes and V. Nemchinsky, *Appl. Phys. Lett.* **73** (1998) p. 1895.
8. A. Shakouri and J.E. Bowers, *Appl. Phys. Lett.* **71** (1997) p. 1234.
9. H. Beyer, A. Lambrecht, E. Wagner, G. Bauer, H. Böttner, and J. Nurnus, *Physica E* **13** (2002) p. 965.
10. S.M. Lee, D.G. Cahill, and R. Venkatasubramanian, *Appl. Phys. Lett.* **70** (1997) p. 2957.
11. T. Borca-Tasciuc, W.L. Liu, T. Zeng, D.W. Song, C.D. Moore, G. Chen, K.L. Wang, M.S. Goorsky, T. Radetic, R. Gronsky, T. Koga, and M.S. Dresselhaus, *Superlattices Microstruct.* **28** (2000) p. 119.
12. G.H. Zeng, A. Shakouri, C. La Bounty, G. Robinson, E. Croke, P. Abraham, X.F. Fan, H. Reese, and J.E. Bowers, *Electron. Lett.* **35** (1999) p. 2146.
13. S. Cho, Y. Kim, S.J. Youn, A. DiVenere, G.K.L. Wong, A.J. Freeman, J.B. Ketterson, L.J. Olafsen, I. Vurgaftman, J.R. Meyer, and C.A. Hoffman, *Phys. Rev. B* **64** 235330 (2001).
14. M.S. Dresselhaus, Y.M. Lin, S.B. Cronin, O. Rabin, M.R. Black, G. Dresselhaus, and T. Koga, *Semicond. Semimetals* **71** (2001) p. 1.
15. J. Nurnus, H. Böttner, and A. Lambrecht, in *Handbook of Thermoelectrics,* edited by M. Rowe, Chapter 46 (CRC Press, Boca Raton, FL, 2005) p. 1.
16. D. Mahan, *Semicond. Semimetals* **71** (2001) p. 157.
17. M.S. Dresselhaus, G. Dresselhaus, X. Sun, Z. Zhang, S.B. Cronin, T. Koga, J.Y. Ying, and G. Chen, *Microscale Thermophys. Eng.* **3** (1999) p. 89.
18. G. Chen, M.S. Dresselhaus, J.-P. Fleurial, and T. Caillat, *Int. Mater. Rev.* **48** (2003) p. 45.
19. G. Chen and A. Shakouri, *J. Heat Transfer* **124** (2001) p. 242.
20. G. Springholz, A. Holzinger, H. Krenn, H. Clemens, G. Bauer, H. Böttner, P. Norton, and M. Maier, *J. Cryst. Growth* **113** (1991) p. 593.
21. A. Lambrecht, H. Böttner, M. Agne, R. Kurbel, A. Fach, B. Halford, U. Schiessl, and M. Tacke, *Semicond. Sci. Technol.* **8** (1993) p. 334.
22. R. Venkatasubramanian, T. Colpitts, B. O'Quinn, M. Lamvik, and N. El-Masry, *Appl. Phys. Lett.* **75** (1999) p. 1104.
23. J. Nurnus, H. Beyer, A. Lambrecht, and H. Böttner, in *Thermoelectric Materials 2000—The Next Generation Materials for Small-Scale Refrigeration and Power Generation Applications,* edited by T.M. Tritt, G.S. Nolas, G.D. Mahan, D. Mandrus, and M.G. Kanatzidis (Mater. Res. Soc. Proc. **626**, Warrendale, PA, 2000) p. Z2.1.1.
24. H. Cui, I. Bhat, B. O'Quinn, and R. Venkatasubramanian, *J. Electron. Mater.* **30** (2001) p. 1376.
25. A. Mzerd, D. Sayah, G. Brun, J.C. Tedenac, and A. Boyer, *J. Mater. Sci. Lett.* **14** (1995) p. 194.
26. A. Mzerd, D. Sayah, J.C. Tedenac, and A. Boyer, *Int. J. Electron.* **77** (1993) p. 291.
27. Y.A. Boikov, V.A. Danilov, T. Claeson, and D. Erts, in *Proc. ICT'97* (IEEE, New York, 1997) p. 89.
28. A. Foucaran, A. Giani, F. Pascal-Delannoy, A. Boyer, and A. Sackda, *Mater. Sci. Eng., B* **52** (1998) p. 154.
29. F. Völklein, V. Baier, U. Dillner, and E. Kessler, *Thin Solid Films* **187** (1990) p. 253.
30. V.D. Das and P.-G. Ganesan, in *Proc. 16th Int. Conf. Thermoelectrics* (IEEE, New York, 1997) p. 147.
31. H. Zou, M. Rowe, and G. Min, in *Proc. ICT'00* (IEEE, Piscataway, NJ, 2002) p. 251.
32. L.W. Da Silva, M. Kaviany, A. DeHennis, and J.S. Dyck, in *Proc. ICT'03* (IEEE, Piscataway, NJ, 2003) p. 665.
33. J. Nurnus, H. Böttner, H. Beyer, and A. Lambrecht, in *Proc. ICT'99* (IEEE, Piscataway, NJ, 1999) p. 696.
34. J.P. Fleurial, L. Gailliard, and R. Triboulet, *J. Phys. Chem. Solids* **49** (1988) p. 1237.
35. H. Böttner, A. Schubert, H. Kölbel, A. Gavrikov, A. Mahlke, and J. Nurnus, in *Proc. ICT'04*, CD-ROM, Paper No. 009 (IEEE, Piscataway, NJ, 2004).
36. F.R. Harris, S. Standridge, C. Feik, and D.C. Johnson, *Angew. Chem. Int. Ed. Engl.* **42** (2003) p. 5295.
37. M. Chitroub, S. Scherrer, and H. Scherrer, *J. Phys. Chem. Solids* **62** (2000) p. 1693.
38. A. Lambrecht, H. Beyer, J. Nurnus, C. Künzel, and H. Böttner, in *Proc. ICT'01* (IEEE, Piscataway, NJ, 2001) p. 335.
39. A. Lambrecht, N. Herres, B. Spanger, S. Kuhn, H. Böttner, M. Tacke, and J. Evers, *J. Cryst. Growth* **108** (1991) p. 301.
40. G. Springholz, V. Holy, M. Pinczolits, and G. Bauer, *Science* **282** (1998) p. 734.
41. H. Zogg and M. Hüppi, *Appl. Phys. Lett.* **47** (1985) p. 47.
42. T.C. Harman, D.L. Spears, and M.J. Manfra, *J. Electron. Mater.* **25** (1996) p. 1121.
43. T.C. Harman, D.L. Spears, D.R. Calawa, and S.H. Groves, in *Proc. 16th Int. Conf. Thermoelectrics* (IEEE, New York, 1997) p. 416.
44. T.C. Harman, D.L. Spears, and M.P. Walsh, *J. Electron. Mater. Lett.* **28** (1999) p. L1.
45. T.C. Harman, P.J. Taylor, D.L. Spears, and M.P. Walsh, *J. Electron. Mater.* **29** (2000) p. L1.
46. H. Beyer, J. Nurnus, H. Böttner, A. Lambrecht, T. Roch, and G. Bauer, *Appl. Phys. Lett.* **80** (2002) p. 1216.
47. J.C. Caylor, K. Coonley, J. Stuart, S. Nangoy, T. Colpitts, and R. Venkatasubramanian, in

Proc. 24th Int. Conf. Thermoelectrics (IEEE, Piscataway, NJ, 2005).
48. N. Peranio, O. Eibl, and J. Nurnus, in *Proc. 23rd Int. Conf. Thermoelectrics* CD-ROM, Paper No. 1059 (IEEE, Piscataway, NJ, 2004).
49. J.C. Caylor, M.S. Dander, A.M. Stacy, J.S. Harper, R. Gronsky, and T. Sands, *J. Mater. Res.* **16** (2001) p. 2467.
50. W.L. Liu, T. Borca-Tasciuc, G. Chen, J.L. Liu, and K.L. Wang, *J. Nanosci. Nanotechnol.* **1** (2001) p. 39.
51. D.W. Song, G. Chen, S. Cho, Y. Kim, and J. Ketterson, in *Thermoelectric Materials 2000—The Next Generation Materials for Small-Scale Refrigeration and Power Generation Applications*, edited by T.M. Tritt, G.S. Nolas, G.D. Mahan, D. Mandrus, and M.G. Kanatzidis (Mater. Res. Soc. Proc. **626**, Warrendale, PA, 2000) p. Z9.1.1.
52. D.W. Song, W.L. Liu, T. Zeng, T. Borca-Tasciuc, G. Chen, C. Caylor, and T.D. Sands, *Appl. Phys. Lett.* **77** (2000) p. 3854.
53. G. Chen, B. Yang, W.L. Liu, T. Borca-Tasciuc, D. Song, D. Achimov, M.S. Dresselhaus, J.L. Liu, and K.L. Wang, *Proc. 20th Int. Conf. Thermoelectrics* (IEEE, Piscataway, NJ, 2001) p. 30.
54. S.M. Lee and D.G. Cahill, *J. Appl. Phys.* **81** (1997) p. 2590.
55. W.S. Capinski, H.J. Maris, T. Ruf, M. Cardona, K. Ploog, and D.S. Katzer, *Phys. Rev. B* **59** (1999) p. 8105.
56. T.C. Harman, *J. Appl. Phys.* **29** (1958) p. 1373.
57. C.R. Tellier and A.J. Tosser, *Size Effects in Thin Films* (Elsevier, Amsterdam, 1982).
58. G. Chen, *J. Heat Transfer* **119** (1997) p. 220.
59. G. Chen, *Phys. Rev. B.* **57** (1998) p. 14958.
60. P. Hyldgaard and G.D. Mahan, *Phys. Rev. B* **56** (1997) p. 10754.
61. S. Tamura, Y. Tanaka, and H.J. Maris, *Phys. Rev. B* **60** (1999) p. 2627.
62. B. Yang and G. Chen, *Microscale Thermophys. Eng.* **5** (2001) p. 107.
63. M.V. Simkin and G.D. Mahan, *Phys. Rev. Lett.* **84** (2000) p. 927.
64. B. Yang and G. Chen, *Phys. Rev. B* **67** 195311 (2003).
65. B.C. Daly, H.J. Maris, K. Imamura, and S. Tamura, *Phys. Rev. B* **66** 024301 (2002).
66. R. Venkatasubramanian, *Phys. Rev. B* **61** (2000) p. 3091.
67. B. Yang and G. Chen, in *Chemistry, Physics, and Materials Science for Thermoelectric Materials: Beyond Bismuth Telluride*, edited by M.G. Kanatzidis, T.P. Hogan, and S.D. Mahanti (Kluwer Academic/Plenum, NY, 2003) p. 147.
68. R. Venkatasubramanian, E. Siivola, B. O'Quinn, K. Coonley, P. Addepalli, C. Caylor, A. Reddy, and R. Alley, *Proc. 24th Int. Conf. Thermoelectrics* (IEEE, Piscataway, NJ, 2005).
69. R. Venkatasubramanian, E. Siivola, B.C. O'Quinn, K. Coonley, P. Addepalli, M. Napier, T. Colpitts, and M. Mantini, *Proc. 2003 ACS Symp. Nanotechnol. Environ.*, ACS Symposium Series **890** (American Chemical Society, Washington, DC, 2004) p. 347.
70. F. Völklein, M. Blumers, and L. Schmitt, *Proc. 18th Int. Conf. Thermoelec.* (IEEE, Piscataway, NJ, 1999) p. 285.
71. J. Nurnus, H. Böttner, C. Künzel, U. Vetter, A. Lambrecht, J. Schumann, and F. Völklein, *Proc. 21st Int. Conf. Thermoelectrics* (IEEE, Piscataway, NJ, 2002) p. 523).
72. R. Alley, J. Canchhevaram, K. Coonley, B. O'Quinn, J. Posthill, E. Siivola, and R. Venkatasubramanian, *Proc. 24th Int. Conf. Thermoelectrics* (IEEE, Piscataway, NJ, 2005).
73. Y.-M. Lin and M.S. Dresselhaus, *Phys. Rev. B* **60** 075304 (2003). □

Advertisers in This Issue

For free information about the products and services offered in this issue, check **http://www.mrs.org/bulletin_ads**
*Please visit us at the Exhibit, April 18–20, during the 2006 MRS Spring Meeting in San Francisco.